Imperfection Photoconductivity in Diamond*

J. A. ELMGREN† AND D. E. HUDSON
Institute for Atomic Research and Department of Physics, Iowa State University, Ames, Iowa
(Received November 8, 1961; revised manuscript received August 3, 1962)

The effect of monochromatic light throughout the visible region on the rate of decay of a persistent internal field in diamond has been studied. The persistent field was generated by spacially-separated trapped electrons and holes, and was sampled by the counting rate of the polarized diamond acting as a nuclear particle counter. Under the influence of light the internal field decayed exponentially with time in a fashion characterized by an intensity-dependent decay constant. The decay constants, normalized to a common photon flux density, varied over more than four orders of magnitude in the photon energy range from 1.8 to 3.5 eV.

The results are interpreted in terms of imperfection photoconductivity arising from imperfection levels with photoionization energies of 2.5 and 3.0 eV. This photoconduction model utilizes a decay mechanism which has been overlooked in previous diamond work. An alternate conventional interpretation in terms of detrapping is also presented.

I. INTRODUCTION

A. Foreword

INTEREST in the nature of the imperfections in diamond has continued for many years. In 1934, Robertson *et al.*[1] proposed a classification of diamonds into two types, type I and type II, on the basis of their optical properties and their photoconductive response to ultraviolet light. Research since that time has made increasingly evident the fact that this classification is too elementary. Experiments on the optical properties indicate the existence of three major imperfections. Some differences in diamond properties can be traced to differences in the amounts of these imperfections. Recently, nitrogen was discovered to be a major impurity[2] in type I diamond. The nitrogen content was found to be correlated with the magnitude of an infrared absorption band which had been correlated[3] with the secondary absorption edge at about 3000 Å. The imperfections associated with optical absorption systems at 4150 Å (3.0 eV) and at 5032 Å (2.5 eV) have not yet been identified. Although the optical properties of these imperfections have been investigated[4] to a considerable extent, their contribution to photoconduction is not established. Knowledge of the spectral response of imperfection photoconductivity in this spectral region would aid in the correct determination of the positions of energy levels in the forbidden gap. Conventional photoconductivity measurements with visible light[1,5] are either impossible or unreliable because the signal is of the same order of magnitude as the dark current and because polarization phenomena disturb the measurement. The purpose of this paper is to report the trend of the photoconductivity in the spectral range from about 1.8 to 3.5 eV. The measurements were made by an unusually sensitive method which is based upon the conduction-counting properties of the crystal. This work is the first on insulating diamond to be made in this spectral range with adequate sensitivity for quantitative interpretation.

B. The Present Experiment

General Method

In this experiment an internal electric field generated by spacially-separated trapped electrons and trapped holes was observed as it decayed in time. The decay was caused by the neutralization of trapped charges by photon-excited carriers. The rate of decay of the internal field was a measure of the rate of excitation of carriers. The basic operation sequence or "run" proceeded as follows:

(1) An internal field was created in the diamond by a method to be described.

(2) The internal field was observed as it decayed under the action of light incident on the diamond.

The whole experiment consisted of many such runs carried out with light of various wavelengths and intensities.

Creation and Sampling of the Internal Field

The general method, given above, requires an observable measure of the internal field. That measure was the counting rate of the diamond acting as a nuclear radiation detector.[6] A brief description of the counting

* Contribution No. 1079. Work was performed in the Ames Laboratory of the U. S. Atomic Energy Commission.
† Present Address: Swarthmore College, Swarthmore, Pennsylvania.
[1] R. Robertson, J. J. Fox, and A. E. Martin, Phil. Trans. Roy. Soc. (London) A232, 463 (1934).
[2] W. Kaiser and W. L. Bond, Phys. Rev. 115, 857 (1959); W. V. Smith, P. P. Sorokin, I. L. Gelles, and G. J. Lasher, *ibid.* 115, 1546 (1959).
[3] G. B. B. M. Sutherland, D. E. Blackwell, and W. G. Simeral, Nature 174, 901 (1954).
[4] C. D. Clark, R. W. Ditchburn, and H. B. Dyer, Proc. Roy. Soc. (London) A234, 363 (1956); H. B. Dyer and I. G. Matthews, *ibid.* A243, 320 (1958); R. J. Elliott, I. G. Matthews, and E. W. J. Mitchell, Phil. Mag. 3, 360 (1958).
[5] B. Gudden and R. W. Pohl, Z. Physik 17, 331 (1923).
[6] Much previous work on the conduction-counting properties of diamond appears in the literature. Review articles have been written by R. Hofstadter, Nucleonics 4, No. 4, 2, and No. 5, 29 (1949); and F. C. Champion, Proc. Roy. Soc. (London) A234, 541 (1956). Other helpful articles are K. G. McKay, Phys. Rev. 74, 1606 (1948); and R. K. Willardson and G. C. Danielson, U. S. Atomic Energy Commission Report ISC-163, 1950 (unpublished).

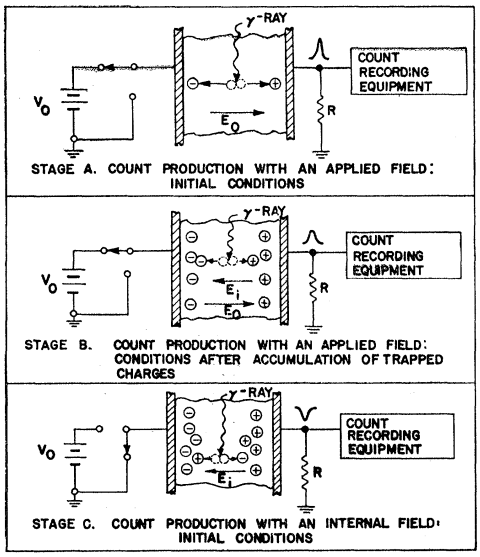

FIG. 1. Representation of counting phenomena during the various stages of the experiment.

properties as they apply to this experiment will help explain the method.

A pictorial representation of the counting phenomena observed in the experiment is shown in Fig. 1. The three parts of the figure represent the diamond at different stages in the sequence of operations in the experiment. The parallel-faced diamond slab is held between two electrodes, one of which is connected to ground through a large resistor, R. The other electrode is connected either to a high-voltage source (V_0) or to ground. Stage A shows the diamond at the start of the experiment, i.e., at the start of the creation of the internal field. The energy of a gamma ray entering the diamond is converted into the creation energy for many electron-hole pairs. Under the influence of the applied field, E_0, the holes and electrons move in opposite directions across the diamond. Their motion continues until they either reach the electrode boundary or become trapped at imperfections. The collective motion of the charges inside the diamond induces a current pulse in the external circuit. This current pulse produces (across R) a voltage pulse which is amplified and, if of sufficient amplitude, is counted by the detection system. The amplitude of the voltage pulse depends on the number of hole-electron pairs formed, the magnitude of the electric field causing drift, and other parameters which are constant for any particular diamond (Hofstader[6] and McKay[6]). The dependence on the magnitude of the electric field is the most important for this experiment. Consider what happens as the gamma rays continue to enter the diamond. As shown in stage B, the trapped holes and electrons generate an internal field, E_i, which opposes the applied field, E_0, to result in a net effective drift field,

$$E_d = E_0 - E_i. \quad (1)$$

Since $E_d < E_0$, the pulse amplitudes, and, therefore, the counting rate (the number of pulses with amplitudes greater than a certain minimum), decreases with time from their initial values. An internal field has thus been created by a counting process. Finally, consider the situation shown in stage C where E_0 has been removed. The internal field is generated by trapped charges and therefore persists. The diamond "counts" under the influence of E_i much as it did under E_d except that the pulses have opposite signs. The internal field may then be sampled in terms of the counting rate.

Under internal-field conditions, the free holes and electrons excited by the γ rays also cause decay of the field by neutralization of the trapped charge. Since the object of the experiment was to observe the decay of internal field caused by light incident on the diamond, this gamma-induced decay was a perturbing effect. Therefore, the internal field was sampled by measuring the counting rate for periods short enough and sufficiently separated to allow the light to have the major effect.

This basic experiment was used to obtain the variation of the internal field counting rate, R_i, with time when light was incident on the diamond. The internal field, and therefore R_i, was expected to decay with time at a rate dependent on the rate of liberation of charge carriers. The rate of liberation of carriers by light was expected to be dependent on both photon energy and photon flux density, so the basic experiment was repeated with different light conditions for each run. A decay constant (equal to the reciprocal of the time constant for a simple exponential decay) characterized the data from each run. These decay constants for different photon energies were compared at a common photon flux density to determine the relative efficiencies of carrier liberation.

II. INSTRUMENTATION

Figure 2 is the block diagram of the experimental apparatus arranged to show the three major parts: the basic counting apparatus, the count recording equipment, and the source of illumination.

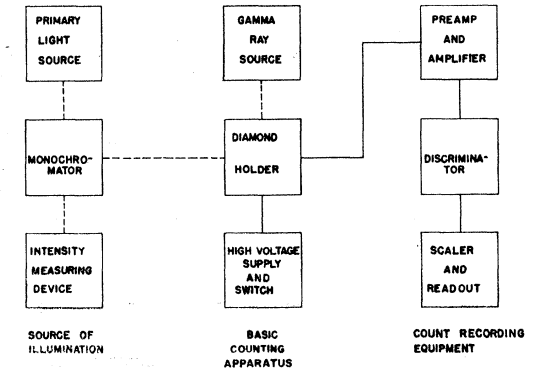

FIG. 2. Block diagram of the experimental apparatus.

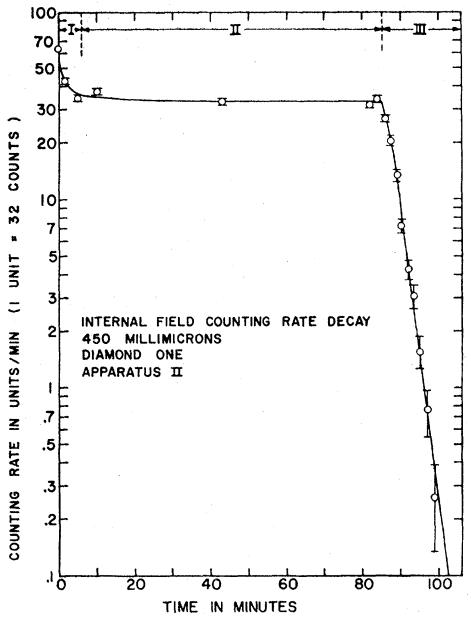

FIG. 3. Sample internal field counting rate decay run for D1. Regions I and II: diamond in dark. Region III: diamond illuminated with 450-mμ light.

The basic counting apparatus is diagrammed in Fig. 1. The gamma radiation came from a half-mC cobalt-60 source which moved freely between an unshielded position to a shielded position behind 3 in. of lead. One electrode on the diamond was the coating on a transparent NESA[7] glass plate and the other was a copper foil. The foil electrode was connected to the preamp input tube. (The grid resistor R was 40 meg.)

A modified Bell-Jordan linear amplifier and preamplifier, a pulse-height discriminator, and a scaler comprised the count recording equipment. The gain of the amplifier and preamp was about 6×10^4 and the pulse-height discriminator was set at 7.0 V.

Steady monochromatic illumination of known wavelength and intensity was supplied by a Bausch and Lomb 250-mm focal-length grating monochromator. The light sources were an Hanovia-type mercury arc and an incandescent lamp. Bandwidths of 10 to 50 Å were used with the discrete lines and of about 40 Å for the visible and ultraviolet; in the near infrared, bandwidths up to 500 Å were required. A front-surfaced aluminum mirror set at 45 deg to the emergent beam from the monochromator directed the beam either to the diamond holder or to an RCA 929 or an RCA 925 photocell. Each photocell used in the experiment was calibrated for relative spectral sensitivity by comparison with a photocell of the same type which had been calibrated by the National Bureau of Standards. Knowledge of the photocurrents at several wavelengths in the 500- to 600-mμ range allowed the relative intensities at all wavelengths to be determined to a standard error of about 7%. Sensitivity data supplied by RCA[8] was used to establish an approximate absolute intensity scale. No result of this work requires that the absolute intensities be known to high accuracy. On the basis of auxiliary measurements with a thermopile we feel that the absolute intensities are reliable to within a factor of 2.

[7] Trade name (Pittsburgh Plate Glass Company, Pittsburgh, Pa.) for a commercially available glass with a conducting surface coating.

III. PROCEDURE

The diamond to be investigated was carefully cleaned before insertion in the diamond holder. A drop of Aquadag improved the electrical contact between the diamond and the foil electrode. After insertion, the diamond was checked for pulses due to electrical breakdown.

The discussion of Sec. I B suggests and introduces the experimental procedure which was followed. The diamond was kept in complete darkness except for the controlled admission of monochromatic light. Each run was initiated by supplying an "applied" field of 10 kV/cm. Immediately, thereafter, the gamma source was moved to its counting position. The counting period with the field applied was about 1 hr, after which the internal field was of sufficient magnitude to proceed with the remainder of the run. The condition is then represented by stage B of Fig. 1.

The transition from the applied field counting condition to the internal field counting condition (stage C, Fig. 1) was made rapidly in order to detect any relatively fast initial decay. (30-sec counting periods were used.) The progress of the internal field decay was observed by sampling the internal field counting rate as a function of time. The criterion for the frequency of sampling was that the amount of decay induced by the gamma rays be negligible.

The internal field decay *in the dark* was observed for about 1 h in order to insure that the "dark-decay" rate was known. This decay rate could be applied as a small correction to the decay rate with illumination. The progress of the internal field decay caused by monochromatic illumination (photon-induced decay) of the diamond also was studied in the manner described.

The final procedure in a complete run was to restore the diamond to the same condition as at the start of the run. Different procedures were employed ranging from retention of the grounded diamond in the dark for 6 hrs or more to bombardment of the grounded diamond by gamma rays for an hour. No correlation between the procedure used and the behavior of the diamond during the subsequent run was observed.

IV. EXPERIMENTAL DATA

Two diamonds have been investigated in this experiment. These were chosen from our collection of counting

[8] RCA Tube Handbook RB-3, Vol. 3-4.

diamonds for their high internal field counting rate.[9] Diamond One (abbreviated D1) was a clear, colorless slab with approximately rectangular faces 4.7 mm by 4.3 mm. These faces were essentially plane and free from visible flaws. The specimen was slightly wedge shaped over its average thickness of 4.5 mm. Diamond Four (abbreviated D4) was free from visible flaws, was clear and colorless, and had flat faces of equilateral triangular shape, about 3.5 mm on a side and 0.7 mm apart. By qualitative optical absorption techniques,[10] D1 was identified as 75 to 90% type II and the remainder type I, while D4 was 25 to 50% type II.

The applied field counting rate, R_a, was determined as a function of time for each run as a check for reproducible results. The time dependence for different runs was similar, and fluctuations of individual runs were not apparently correlated with fluctuations in the final experimental results. Some difference in the applied field behavior of the two diamonds corresponded to differences which will be noted in the internal field counting rate data.

The internal field counting rate data are those of major interest in this experiment. About 30 runs were taken on each diamond. Presentation of all the data is impractical, but synopses will be presented in connection with Sec. V. Instead, the graph of a sample run for each diamond will be discussed. Run-to-run fluctuations occurred in both the shape and counting rate level of the decay curves. However, the fluctuations were sufficiently small that a sample run can be discussed with the assurance that the qualitative features of all runs for that diamond will be described.

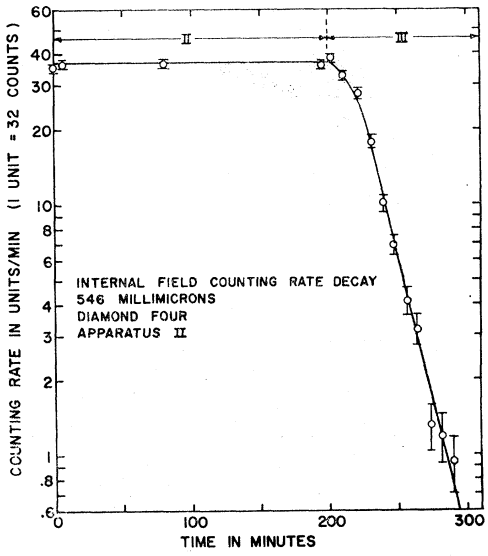

FIG. 4. Sample internal field counting rate decay run for D4. Region II: diamond in dark. Region III: diamond illuminated with 546-mμ light.

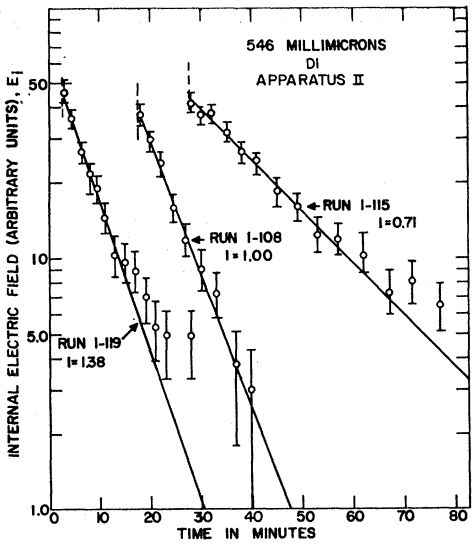

FIG. 5. Examples of converted photon-induced decay data for D1. The relative intensities, I, are given.

Figures 3 and 4 are plots of the internal field counting rate, R_i, versus the time elapsed from the start of the decay. For D1, region I shows a fast initial decay of R_i with the diamond in the dark. No fast initial decay was observed with D4. The diamond remained in the dark throughout the slow dark decay shown in region II. The photon-induced decay is shown in region III. The standard error bars represent the effect of counting statistics only. The decay in the dark (regions I and II) for any one diamond was similar for all runs, whereas the photon-induced decay (region III) varied with both wavelength and intensity of the illumination. This last variation was restricted to the rate of decay; the shape was relatively free from change. A curvature exists in the high counting rate data in region III in these plots. At the lower counting rates, the decay shape appears to be a simple exponential. A strict proportionality between counting rate and electric field is expected only for small fields. The fact that a substantially exponential photon-induced decay is observed supports a *simple* model of the decay mechanism.

V. DATA ANALYSIS

A. Introduction

The sample plots (Figs. 3 and 4) show the decay of the counting rate with time. However, the important variable is actually the internal electric field. The counting rate is strictly proportional to the internal electric field only for small fields; a conversion from R_i to E_i is therefore desirable. This conversion was accomplished through an experimentally determined graph of counting rate vs net electric field. The auxiliary experiment by which the data for this graph were determined

[9] The supplier was Louis Small, President of the Diamond Service Tool Comapny.

[10] R. K. Willardson and G. C. Danielson, J. Opt. Soc. Am. 42, 42 (1952). (D1 is designated as FSC-5 in this reference.)

is decribed in Appendix A. The converted photon-induced decay region (region III) of three runs on D1 are shown in Fig. 5. These runs were taken with different relative intensities (I) for the same wavelength. For D1, the tendency of converted E_i values to level off at a finite value was common. This effect arises from experimental uncertainties involved in the conversion and is not believed to be real. The region III plots of $\ln R_i$ vs the time (t) (Figs. 3 and 4) were generally slightly curved at the higher counting rates. As expected, the conversion removed the curvature at the expense of accuracy at the lower counting rates. The higher counting rate data are considered to be the most reliable. A similar plot of converted data for D4 is shown in Fig. 6. The error bars assigned to the points are combinations of the errors involved in conversion and the counting rate errors from the unconverted data. The characteristic quantity for these data was taken to be the decay constant, b_p. This decay constant is defined as the absolute value of the slope of the straight line portion of the converted photon-induced decay plot. A standard error of the decay constant was estimated from data graphs similar to Figs. 5 and 6. A synopsis of all of the data after analysis in terms of the effective internal field E_i is given in Appendix B. It should be noted that an analysis of the unconverted data of low counting rates yielded decay constants which agreed within a factor of two with the decay constants obtained from the converted data.

It must be emphasized that the existence of a meaningful decay constant for the processes studied is most crucial and has been clearly demonstrated by this experiment. This rather gratifying behavior of diamond in a rather complex situation suggests that a reasonably simple interpretation may be available.

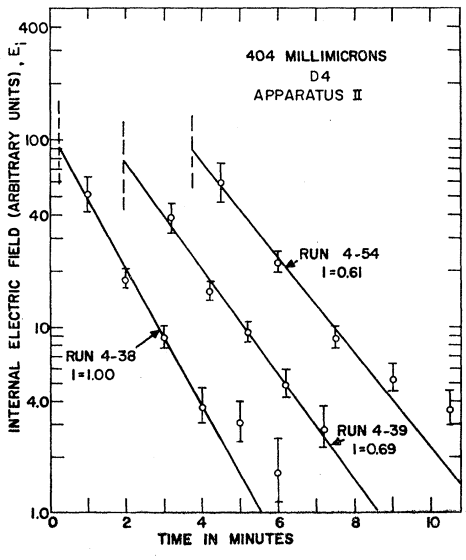

FIG. 6. Examples of converted photon-induced decay data for D4. The relative intensities, I, are given.

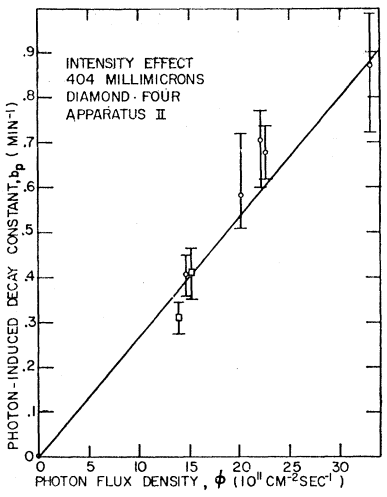

FIG. 7. Sample plot of the effect of photon flux density on the decay constant. The circles represent data taken with the mercury arc source. The squares represent data taken with the 1000-W incandescent source at the same nominal wavelength (404 mμ).

B. Dependence of b_p on Photon Flux

A sample plot of b_p vs ϕ at one photon energy is shown in Fig. 7. The error flags represent the standard error in b_p. The origin is an experimental point on this scale. Similar plots were made for each photon energy. Scatter in the data varied from plot to plot in an apparently random manner. The conclusion derived from a consideration of all plots was that b_p was linearly related to ϕ for the fluxes used. The slope, $\Delta b_p/\Delta\phi$, for each plot was determined from the best straight line through the data. A standard error in each slope was assigned from the uncertainty in the relative ϕ's and from the scatter in the data.

The lack of appreciable saturation effects in the intensity dependence of b_p is another crucial result and is necessary for the analysis to proceed in a straightforward fashion.

C. Dependence of b_p on Photon Energy

The final step in the analysis was to plot b_p as a function of photon energy, W. A meaningful analysis requires that the b_p values be normalized to a common flux density ϕ_c. The normalized decay constant B was calculated from $B=(\Delta b_p/\Delta\phi)\phi_c$, where ϕ_c was 10^{16} cm^{-2} sec^{-1}. Semilogarithmic plots of B vs W for each diamond are shown in Figs. 8 and 9. The two diamonds appear to exhibit very similar dependences of B on W over four orders of magnitude. The absolute values of B are different as may be expected since two diamonds do not necessarily have the same imperfection content. The most rapid variation of B is in the energy range from 1.9 to 2.5 eV. The variation above 2.5 eV is more gradual. A peak around 3.3 eV is weakly suggested for D4. The error bars represent the standard error of

$\Delta b_p/\Delta\phi$ combined with the uncertainty in the relative spectral sensitivity of the photocell. Uncertainties regarding the *absolute* photon fluxes have no effect on these results.

VI. INTERPRETATION

A. Qualitative Features

The interpretation of the data and results presented here is based on the assumption that the counting rate observed in the absence of an applied electric field is a result of a persistent internal electric field generated by trapped charges in the diamond. This assumption is consistent with the observations of this experiment. The decrease in the internal field is caused by the neutralization of the trapped charges by their charge-opposites. Neutralization follows liberation of charge carriers from two possible sources: energy levels filled by trapping during the initial counting period with an applied electric field, and energy levels normally full in the unperturbed neutral diamond. Both of these sources will be used in this interpretation.

The internal field is observed to decay in the dark (regions I and II of Figs. 3 and 4). This decay is interpreted as resulting from the liberation of trapped charges by thermal agitation. In this interpretation, the fast initial decay (region I) is caused by excitation from shallow traps; the slower decay (region II), from deeper traps. The absence of the fast decay in D4 implies that very shallow traps, if any, are emptied thermally in times too small to be seen in this experiment.

The photon-induced excitation of charge carriers from normally full levels is assumed responsible for the decay of E_i during illumination of the diamond (region III).

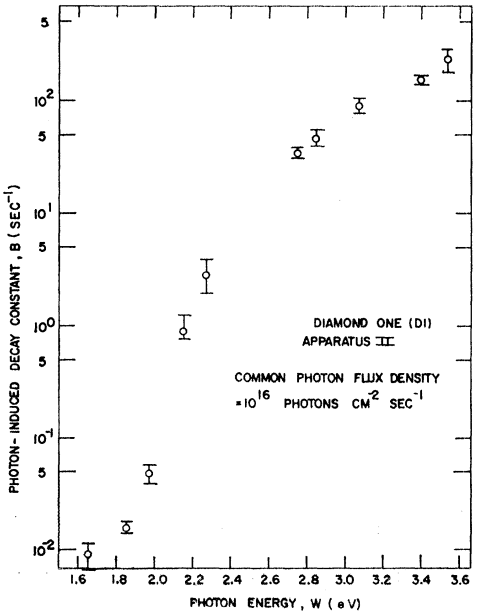

FIG. 8. Variation of the photon-induced decay constant with photon energy for D1.

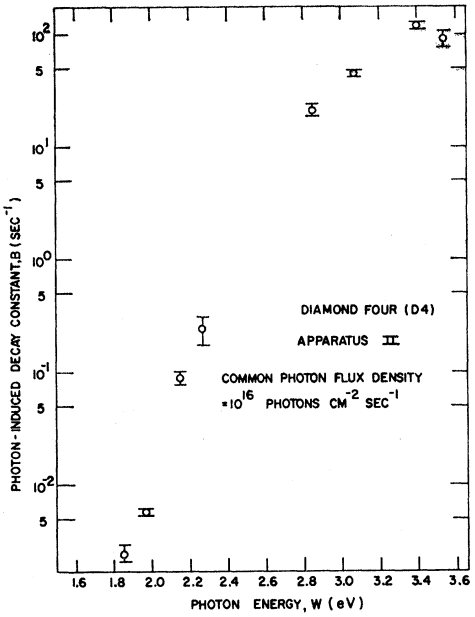

FIG. 9. Variation of the photon-induced decay constant with photon energy for D4.

The conduction process originating with the excitation is known as imperfection photoconduction.[11] Normally full imperfection levels instead of levels filled by trapping were chosen as the source of carriers because this choice more adequately correlated with known properties of diamond. Specifically, experiments on optical absorption and luminescence have shown the existence of optical systems beginning at 4135 Å (3.0 eV) and 5032 Å (2.5 eV) in both type I and type IIa diamonds.[4,12,13] The graphs (Figs. 8 and 9) of the experimental results suggest a break in the 2.4–2.6-eV range and in the case of D4 a possible maximum in the 3.2-eV region. The correlation of these energies with those of known optical systems is considered significant evidence for the present interpretation.

B. Band Model and Decay Mechanisms

The qualitative interpretation just presented requires four energy levels: two trapping levels and two normally full imperfection levels. No data which allow the assignment of these levels to holes or electrons appear to exist; internally consistent but somewhat arbitrary assignments will be made, therefore, for the present to simplify the interpretation. An important point in the choice of a model is that both electrons and holes must be trapped in order that the internal field will persist after the applied field is removed.

---

[11] R. H. Bube, *Photodonductivity of Solids* (John Wiley & Sons, Inc., New York, 1960), Chap. 6, p. 129.

[12] C. Bull and G. F. J. Gailick, Proc. Phys. Soc. (London) **A63**, 1283 (1950).

[13] N. G. Trott, Proc. Roy. Soc. (London) **A220**, 498 (1953).

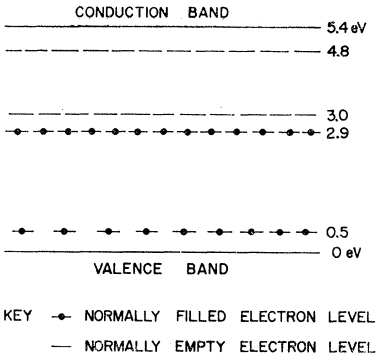

FIG. 10. Possible energy levels in unperturbed diamond proposed for the interpretation of this experiment.

The energy band scheme assumed for this interpretation is shown in Fig. 10. The level at 0.5 eV serves as a hole trap, while that at 4.8 eV is an electron trap (trap depth ~0.6 eV). The placement of these levels is consistent with published results on other diamonds.[10,12,13] The filled levels at 2.9 and 3.0 eV, while also serving as hole and electron traps, respectively, are the main sources of electrons and holes for the photon-induced decay portion of the experiment.[14]

The situation after an internal field has been created is represented in Fig. 11. The figure shows the band scheme at two different positions in the diamond. The position denoted by the left scheme was near the anode when the external field was applied. Therefore electrons (circled minus signs) were trapped in this region. The scheme on the right was near the (original) cathode. Holes (circled plus signs) were trapped in this region. The decay mechanisms are also shown in this figure. Transitions are indicated by vertical dotted arrows and the subsequent motion is indicated by the direction of the horizontal solid arrows. Process 1 is the thermal excitation of a hole to the valence band in which the hole is free to move under the influence of the internal field E_i. The hole moves to neutralize the trapped electrons. This process is responsible for the fast initial dark decay (region I). The slower dark decay (region II) is caused by process 2; thermal excitation of a trapped electron to the conduction band followed by motion of the electron and neutralization of a trapped hole. Processes 3 and 4 are responsible for the photon-induced decay data. Process 3 is the photo-excitation of an electron from a normally full level to the conduction band. Process 4 is the photo-excitation of a hole. The photo-excitation of the *trapped* electrons and holes from deep levels is also possible, but the trapped population is quite small in comparison with the normal population of these levels. (This fact is discussed further in Sec. VI D.) The effect of such excitations on b_p should then also be small. However, at least part of the relatively small response to photons of energy less than about 2.4 eV (Figs. 8 and 9) could be due to this detrapping process from the deep level.

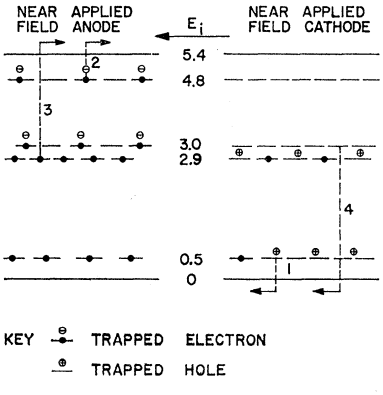

FIG. 11. Mechanisms for the decay of an internal field in diamond. Process 1, detrapping of a hole. Process 2, detrapping of an electron. Process 3, photoexcitation of an electron. Process 4, photoexcitation of a hole.

As in many experiments on diamond, alternate interpretations in terms of "mirrored" energy level positions and of inversions of the roles of holes and electrons can be made to explain the same data. Furthermore, the processes described in the previous paragraphs and their charge alternates may possibly occur simultaneously. However, the relative roles of holes and electrons are unknown. Nothing is to be gained by an overcomplication of the level scheme when the proposed scheme is adequate for understanding the present results and is consistent with other information from trapping, absorption, and luminescence experiments. Hence, the energy level scheme presented in Fig. 10 is intended to be neither a rigid nor a complete band scheme for diamond. Other levels are known to exist.[2] The scheme is presented to explain the results of this experiment in a fashion consistent with other published data. The general scheme is similar to that proposed by Champion,[6] but significant changes based on the results of experiments[4] not available to him have been made.

C. Quantitative Interpretation

The two different quantitative analyses to be given correspond to the two different decay processes: thermal excitation from traps and photoexcitation from normally full levels.

Thermal Detrapping

Let P be the probability per second of liberation of a given trapped charge. If one assumes no retrapping, the rate of change of the number, N_t, of trapped charges is given by $d(\ln N_t)/dt = -P$. If E_i is assumed directly proportional to N_t, then the decay constant for the internal field decay is equal to P. Randall and Wilkins[15] have given an expression for P: $P = S \exp(-W/kT)$, where S is the attempt-to-escape frequency, W is the trap depth, and T is the absolute temperature. Bull and Garlick[12] estimated S to be of the order of 10^6 sec^{-1}.

[14] It has also been suggested that the 2.9- and 3.0-eV levels might be interpreted as a single, partially occupied level lying near the Fermi level.

[15] J. T. Randall and M. H. F. Wilkins, Proc. Roy. Soc. (London) A184, 366 (1945).

Estimates of the decay constants from Regions I and II of Figs. 3 and 4 give trap depths of approximately 0.5 and 0.6 eV, in reasonable agreement with previously reported values.[10,12,13]

More extensive experiments[16] on the dark decay have suggested that the true bulk resistivity of diamond may be several orders of magnitude higher than previously reported.[17]

Photoconductivity

The quantitative analysis of the photon-induced decay is based on the relaxation theory[18] of a homogeneous dielectric medium with a small conductivity. A photoconductivity, σ_p, is assumed to describe the process of interest. Two assumptions are necessary: that $j=\sigma_p E$, where j is the current density and E is the electric field, and that the dielectric constant (K) and σ_p do not vary with position. The validity of the first assumption has not been established with certainty. However, for small electric fields, the photocurrent in the ultraviolet has been observed to vary linearly with applied voltage.[19] The second assumption is probably valid because the light absorption in this spectral range is small and the density of excited carriers is about constant. The theory predicts that $\nabla\cdot\mathbf{E}=(\nabla\cdot\mathbf{E})_{t=0}\times\exp(-\sigma_p t/K\epsilon_0)$ in rationalized MKS units. Since only the time variation is of interest, one finds that the internal field should decay exponentially with a decay constant which is identified with b_p, so that $b_p=\sigma_p/K\epsilon_0$. The photoconductivity (process 3, Fig. 11) may be expressed as $\sigma_p=ne\mu$, where n is the steady state density of photon-liberated electrons, and μ is the mobility of the carriers. According to Rose,[20] the most general relation characterizing photoconductivity is $n=fT$, where f is the excitation rate per unit volume and T is the lifetime of the carriers in the free states. Now $f=N\Sigma\phi$, where N is the density of imperfection centers from which a carrier may be liberated, Σ is the cross section for the liberation process, and ϕ is the photon flux density. Combination of the last four expressions yields

$$b_p=(e\mu T/K\epsilon_0)(N\Sigma)\phi. \tag{2}$$

The linear dependence of b_p on ϕ predicted by this theory was observed in the present experiment. For the common photon flux density, ϕ_c, the experimental parameter B is given by

$$B=(e\mu T/K\epsilon_0)(N\Sigma)\phi_c. \tag{3}$$

The variation of B with photon energy, W, denotes the change in $N\Sigma$ with W. If the wavelength of incident light is such that the absorption coefficient, α, for that light is small, and if the photoconduction transition accounts for all of the absorption, then $\alpha=N\Sigma$. In this case, B should be directly proportional to α. Comparison of the spectral dependence of B with "typical" absorption results[4] were inconclusive; however, the tendency was for B to follow more closely the spectral dependence of the α for a type I diamond than that for type IIa. An estimate of α can be calculated from (3). For diamond, $K=5.67$ and $\mu\sim10^3$ cm^2 V^{-1} sec^{-1};[21] the carrier lifetime is taken to equal τ, the mean free time before trapping. The value of τ from counting experiments[22] is of the order of 10^{-8} sec. At 3.5 eV, α was found to be 0.5 cm^{-1}. It is concluded that some correlation of B and α is suggested by the present experiment (but not confirmed by independent absorption data).

TABLE I. Specific photoconductivity estimates for type IIa diamonds.

W (eV)	C for D1 (mho cm^2 sec)	C for D4 (mho cm^2 sec)
1.85	1.14×10^{-29}	1.7×10^{-30}
1.97	2.4×10^{-29}	2.9×10^{-30}
2.27	9.1×10^{-28}	7.5×10^{-29}
3.07	7.5×10^{-27}	3.8×10^{-27}
3.40	8.8×10^{-27}	6.8×10^{-27}

Aside from any assumed relation between B and α, a numerical estimate of the photosensitivity may be determined from the results. The specific photoconductivity, C, will be defined as the photoconductivity per unit absorbed photon flux: $C=\sigma_p/\alpha\phi$. In this experiment,

$$C=\frac{B}{\phi_c}\frac{K\epsilon_0}{\alpha}.$$

Exact values of C may not be determined because no optical absorption data on $D1$ and $D4$ are available. However, "typical" data[4] for type IIa diamonds were used to estimate the values of C given in Table I.

D. Alternate Interpretation of Photon-Induced Decay

Although the authors believe that the photoconductivity model is the more credible, an alternate model, liberation from deep traps, deserves mention since this model frequently has been suggested to account for qualitative features of the influence of light on diamond conduction counters.

[16] J. A. Elmgren and D. E. Hudson (to be published).
[17] J. A. Elmgren and D. E. Hudson, Bull. Am. Phys. Soc. **6**, 303 (1961).
[18] W. K. H. Panofsky and M. Phillips, *Classical Electricity and Magnetism* (Addison-Wesley Publishing Company, Inc., Reading, Massachusetts, 1955), Chap. 7, p. 111.
[19] F. C. Nix, Revs. Modern Phys. 4, 723 (1932).
[20] A. Rose, *Proceedings of the Photoconductivity Conference, Atlantic City, 1954.* (John Wiley & Sons, Inc., New York, 1956), p. 3.
[21] T. S. Moss, *Photoconductivity in the Elements* (Academic Press Inc., New York, 1952), pp. 101–2.
[22] E. A. Pearlstein and R. B. Sutton, Phys. Rev. **79**, 970 (1950).

The analysis is similar to that employed previously. For the photon excitation, however, $P=\Sigma_t\phi$, where Σ_t is now the cross section for the liberation of a *trapped* charge carrier and ϕ is the photon flux density. The experimental b_p is now identified with P, and for the common photon flux density, ϕ_c, $B=\Sigma_t\phi_c$. The variation of Σ_t with photon energy W is then given by the variation of B with W. The observed cross sections ($\phi_c=10^{16}$ cm^{-2} sec^{-1}) are given in Table II.

The largest cross sections observed in this experiment are of the order of 10^{-14} cm^2 and the smallest are about 10^{-19} cm^2. The small cross sections do not cause concern because the associated transitions may be energetically unfavorable. Geometrical cross sections as large as 10^{-14} cm^2 involve a large number of atom sites. The large cross sections which occur at photon energies above 3.0 eV support a model proposed by Champion,[6] who assumed that aggregates of vacant sites can form in the diamond. The electrons which would normally join in the covalent bonds to the now missing atoms are bound less tightly, accounting for the 2.9-eV level. This center would act predominantly as a hole trap with a large geometrical cross section which might be reflected in a large liberation cross section. The fact that the observed cross section is large for energies greater than 3.0 eV is consistent with the energy level scheme of Champion.

TABLE II. Observed cross sections for liberation of trapped charges.

W (eV)	Σ_t for D1 (cm^2)	Σ_t for D4 (cm^2)
1.85	$(1.59\pm0.20)\times10^{-18}$	$(2.4\ \pm0.4\ )\times10^{-19}$
1.97	$(4.7\ \pm1.0\ )\times10^{-18}$	$(5.71\pm0.34)\times10^{-19}$
2.15	$(9.0\ \pm1.6\ )\times10^{-17}$	$(9.0\ \pm1.2\ )\times10^{-18}$
2.27	$(2.9\ \pm1.0\ )\times10^{-16}$	$(2.4\ \pm0.6\ )\times10^{-17}$
2.85	$(4.7\ \pm0.8\ )\times10^{-15}$	$(2.08\pm0.24)\times10^{-15}$
3.07	$(8.8\ \pm1.4\ )\times10^{-15}$	$(4.41\pm0.34)\times10^{-15}$
3.40	$(1.53\pm0.14)\times10^{-14}$	$(1.18\pm0.10)\times10^{-14}$
3.54	$(2.3\ \pm0.6\ )\times10^{-14}$	$(9.1\ \pm1.5\ )\times10^{-15}$

Although the interpretation just presented is an attractive one, difficulties arise when it is considered carefully. A minor problem with this interpretation is the assumption that $E_i=KN_t$, where K is a constant independent of time. The internal field is a function of both the amount and the distribution of the trapped charge. The distribution is lumped into the constant K, and could possibly be time-dependent because of retrapping.

The major difficulty with this interpretation is that the existence of photoconduction arising from normally filled levels (Sec. VI D) is ignored. The rate of excitation of electrons from the normally full level (process 3, Fig. 9) is probably greater than the rate of detrapping of holes from the same level acting as a trap. The population of the normally full level is (typically) of the order of 10^{15} or 10^{16} cm^{-3}. The number of *trapped* charges required to generate the observed internal fields depends on the spacial distribution of filled traps, which, in turn, depends on the mean displacement of carriers before trapping. If most of the charge is near the crystal surfaces, then only about 10^{10} charges per cm^2 are required. For a uniform internal polarization involving a mean charge separation of, say, 10^{-3} cm (a lower limit estimated from *Schubweg*[6] data), the required density is about 10^{13} cm^{-3}. Since the rate of decay of the internal field is certainly dependent on the rate of charge excitation, which is in turn related to the level population, one would expect to observe the photoconduction process more easily than the detrapping process. Then, one would assign the largest decay constants to photoconduction processes.

VII. DISCUSSION

This experiment is the first to obtain quantitative results for the relative ability of different wavelengths of light to cause the decay of an internal field in diamond. The data were characterized by a decay constant which varied over four orders of magnitude in the range of photon energies from 1.8 to 3.5 eV. The nature of the variation suggested the excitation of carriers to an energy band by photons of energy equal to about 2.5 eV.

The authors have interpreted the results in terms of imperfection photoconductivity. An imperfection level with a photo-ionization energy of 2.5 eV and possibly one with a photo-ionization energy of 3.0 eV are assumed to be responsible for the observed spectral dependence of the photoconductivity. In these terms the experiment extends photoconductivity data on diamond in some detail to the visible wavelengths.

The interpretation of the experiment in terms of imperfection photoconductivity represents a shift in the analysis usually applied to this type of experiment. The decay of the current or the electric field in a polarized material is commonly associated only with a detrapping mechanism. While deep trapping levels are required to understand the persistence of the polarization, the mechanism for the decay should not be limited to detrapping.

When the results of this experiment are compared with those of some reported experiments[1,10,19,23] on the effect of red light on photoconducting and counting diamonds, an apparent contradiction to our results is found. In these latter experiments, both the photoconducting and counting response have been shown to increase with red light illumination concomitant with the exciting radiation (either ultraviolet light or nuclear radiation). The phenomenon has been ascribed to detrapping. Champion and Dale[23] suggested that the red light (2.0 eV) emptied traps which had a smaller thermal depth (they suggested 0.8 eV). If this proposed optical-thermal depth discrepancy is adopted, the apparent contradiction can be explained. The difference lies in the

[23] F. C. Champion and B. Dale, Proc. Roy. Soc. (London) A234, 419 (1956).

different procedures used in the experiments. In this experiment thermal excitation from shallow traps occurred before the diamond was illuminated. The traps normally emptied by red light may have been emptied thermally before the light was applied. The thermal depth of the trap would have to be less than 0.6 eV for this explanation to be reasonable. The contradiction may be resolved by another consideration. The previous work compared the response to red light before and after irradiation by shorter wavelength radiation. The present experiment compares the response to various wavelengths with the diamond in approximately the same condition for each wavelength. Thus, it is possible that there is an additional response after irradiation which is, however, still smaller than the response to shorter wavelength radiation.

ACKNOWLEDGMENTS

The authors wish to acknowledge the contributions of Dr. G. C. Danielson to the work. The methodology of the present study arose from his suggestion for a possible investigation of very shallow traps in the infrared. His continued interest and encouragement were very gratifying.

Several discussions with Dr. V. A. Fassel and R. Kniseley were helpful in the light intensity measurements.

H. Sample and R. Girvan assisted in the construction of gear and in the analysis of the data.

APPENDIX A

The determination of the relation of counting rate to net electric field was accomplished by a straightforward method. The desired data were the internal field counting rate, R_i, vs the internal field, E_i. Since a direct measurement of E_i was impossible, an indirect measure was used. The critical assumption was made that the counting rate is the same function of E_i alone that it is of an applied electric field, E_0, in the absence of E_i. The desired data could then be obtained by recording the initial counting rate at various values of applied field. The problem of "dark polarization" as discussed by Pearlstein[24] made the actual determination less certain, but an attempt was made to compensate for the polarization. Since polarization was present, the observed counting rate, R_0, was due to a net drift field $E_d=E_0-E_i$. A determination of R_i due solely to E_i was made immediately after the R_0 measurement. An iterative technique allowed the correction of E_0 to the net field. The plot of R_0 vs net field was taken as the desired conversion graph.[25]

[24] E. A. Pearlstein, Ph.D. dissertation, Carnegie Institute of Technology, 1950 (unpublished).

[25] Further treatment of this point may be found in J. A. Elmgren, Ph.D. thesis, Iowa State University, Ames, Iowa, 1960 (unpublished).

APPENDIX B

TABLE III. Synopsis of photon-induced decay data on D1.

Photon energy (eV)	Run No.	Photon-induced decay constant b_p (min^{-1})	Photon flux density ϕ (10^{12} cm^{-2} sec^{-1})
3.54	1–124	0.214±0.029	0.201
	1–120	0.64 ±0.14	0.369
3.40	1–112	0.096±0.015	0.108
	1–114	0.259±0.028	0.278
3.07	1–118	0.117±0.015	0.248
	1–116	0.28 ±0.04	0.436
2.85	1–132	0.109±0.012	0.589
	1–123	0.077±0.007	0.216
	1–111	0.195±0.025	0.608
	1–110	0.40 ±0.04	1.21
2.75	1–122	0.067±0.006	0.312
	1–121	0.226±0.026	1.09
2.27	1–115	0.050±0.006	4.68
	1–108	0.123±0.012	6.55
	1–119	0.138±0.017	9.05
	1–135	0.116±0.018	10.3
	1–107	0.39 ±0.06	11.9
2.15	1–117	0.050±0.007	6.64
	1–109	0.025±0.003	8.69
	1–113	0.180±0.026	24.8
2.08	1–131	2.7 ±1.4	791
1.97	1–130	0.078±0.022	346
	1–126	0.31 ±0.12	893
1.85	1–129	0.041±0.007	420
	1–127B	0.085±0.012	883
1.65	1–128	0.017±0.005	675
	1–125	0.10 ±0.12	1420
	1–128	0.023±0.015	670

TABLE IV. Synopsis of photon-induced decay data on D4.

Photon energy (eV)	Run No.	Photon-induced decay constant b_p (min^{-1})	Photon flux density ϕ (10^{12} cm^{-2} sec^{-1})
3.54	4–42	0.25 ±0.06	0.448
	4–52	0.61 ±0.12	1.12
3.40	4–37	0.314 ±0.027	0.481
	4–40	0.70 ±0.08	0.979
	4–35	0.76 ±0.12	0.926
3.07	4–54	0.58 ±0.11	2.03
	4–55	0.31 ±0.04	1.40
	4–53	0.41 ±0.06	1.53
	4–34	0.41 ±0.05	1.48
	4–39	0.68 ±0.06	2.27
	4–38	0.87 ±0.13	3.31
	4–33	0.70 ±0.09	2.23
2.85	4–41	0.34 ±0.04	2.37
	4–48	0.45 ±0.05	3.76
	4–27	0.31 ±0.05	2.87
	4–36	0.69 ±0.07	4.63
	4–26	0.63 ±0.10	5.82
2.27	4–28	0.0025±0.0017	2.72
	4–28	0.0049±0.0020	5.29
	4–29	0.013 ±0.004	14.2
	4–28	0.048 ±0.003	18.0
	4–30	0.041 ±0.007	33.8
	4–31	0.041 ±0.007	36.7
	4–29	0.077 ±0.014	44.5
2.15	4–43	0.013 ±0.004	32.1
	4–43	0.054 ±0.005	107
	4–44	0.113 ±0.014	179
1.97	4–45	0.0219±0.0025	690
	4–46	0.0286±0.0028	860
1.85	4–45	0.0115±0.0027	644
	4–47	0.0199±0.0025	1500
1.65	4–45	0.0058±0.0024	525